Low Temperature Disordered Phase of α-Pb/Ge(111)

Jiandong Guo,[1] Junren Shi,[2] and E. W. Plummer[1,2]

[1]*Department of Physics and Astronomy, The University of Tennessee, Knoxville, TN 37996, USA*
[2]*Condensed-Matter Science Division, Oak Ridge National Laboratory, Oak Ridge, TN 37831, USA*

(Received 4 August 2004; published 26 January 2005)

A new structural phase transition has been observed at low temperature for the one-third of a monolayer (α phase) of Pb on Ge(111) using a variable-temperature scanning tunneling microscope. The well-known $(\sqrt{3} \times \sqrt{3})R30\,^\circ$ to (3×3) transition is accompanied by a new structural phase transition from (3×3) to a disordered phase at $\sim$76 K. The formation of this ''glasslike'' phase is a consequence of competing interactions on different length scales.

DOI: 10.1103/PhysRevLett.94.036105 PACS numbers: 68.35.Rh, 68.35.Bs, 68.37.Ef

Two-dimensional (2D) metallic films on semiconducting substrates are inherently susceptible to structural and electronic transitions because there are competing interactions with different length scales. The long-range electron-mediated indirect interaction drives surface reconstruction, but the interaction with the substrate prefers local order. The structure at any temperature is essentially a balance between these two driving forces and is predicted to lead to a ''glassy'' phase at low temperatures [1]. This behavior is very similar to recent theoretical predictions for phase transitions in correlated electron systems, where there is a competition between interactions on different length scales [2,3] or competition between different order parameters [4]. Indigenous to all these models are ''glasslike'' phases. Here, we report on the observation of a disordered, glasslike phase at low temperature for an ultrathin metallic film of Pb on a Ge(111) surface. In general, the electron-electron and electron-phonon coupling are enhanced in these films due to the reduction of symmetry, making these systems ideal for testing concepts applicable to the correlated electron materials.

The system studied here is one-third of a monolayer of Pb adatoms atop of the Ge(111) surface (α-phase Pb/Ge interface) [5]. It has been reported that the room temperature (RT) $(\sqrt{3} \times \sqrt{3})R30\,^\circ$ structure [referred to as $(\sqrt{3} \times \sqrt{3})$ in the following] undergoes a transition to a (3×3) structure at $T \sim 120$ K. The (3×3) results from an ordered array of *one up-two down* configuration of the Pb atoms. This phase transition in Pb/Ge and in the isoelectronic Sn/Ge interface [6] has been a subject of extensive experimental and theoretical investigation [7–14]. There is still discussion concerning the origin of this transition, especially when the role of defects is included [15–17]. This Letter reports a variable-temperature scanning tunneling microscope (STM) discovery of a new disordered phase upon cooling the sample to below 76 K. In this new phase, the Pb adatoms distort with no apparent long-range order (LRO), resulting in an irregular ''kinked line'' structure. Although defects blur both phase transitions (as they did in the Sn/Ge system [16,18]), it is demonstrated by direct STM imaging that the observed disordered phase is intrinsic to the Pb/Ge interface. The disordered or glasslike phase results from the competition between different interactions in correlated electron systems.

The experiments were performed in an Omicron ultrahigh vacuum variable-temperature STM. The Ge(111) substrate was cleaned *in situ* by repeated sputtering and annealing cycles until nice $c(2 \times 8)$ surface reconstruction was obtained. Pb was deposited from a commercial Knudsen cell (K-Cell) for 45 sec. During deposition the temperature was stabilized at 550 °C in the K-Cell and at 100 °C on the substrate, respectively. Finally, the sample was annealed at 360 °C for 20 min. Well-ordered interface with exact Pb coverage of one-third of a monolayer was verified by the sharp $(\sqrt{3} \times \sqrt{3})R30\,^\circ$ low energy electron diffraction patterns that appeared as soon as the preparation finished. Low temperature (LT) low energy electron diffraction was also performed by cooling the sample with liquid nitrogen. With an onset at 250 K, extra diffraction spots corresponding to (3×3) symmetry became visible and intensified at decreased temperature. This structural transition is gradual and reversible. RT STM images revealed the existence of Ge substitutional defects and negligible amount of vacancies on the $(\sqrt{3} \times \sqrt{3})$ reconstructed surface. By optimizing the post-evaporation annealing temperature and time, the defect density was minimized to about 10% with average distance of about 2 nm between nearest neighboring defects. The sample was then cooled on the STM stage by using a continuous flow cryostat. Temperature at the sample surface was controlled and stabilized in the range between RT and 40 K. All the STM images presented in this Letter were obtained with the tip bias at +1.5 V (filled state) and feedback current at 3 nA. Since the filled-state images are insensitive to the tip bias, it is assumed that these high-bias images mirror the structural information of the Pb/Ge interface directly.

Figures 1(a)–1(c) summarize the STM observation of the Pb/Ge interface at different temperatures. The RT image [Fig. 1(a)] reveals the $(\sqrt{3} \times \sqrt{3})$ structure with the dark spots being the substitutional Ge atoms [15].

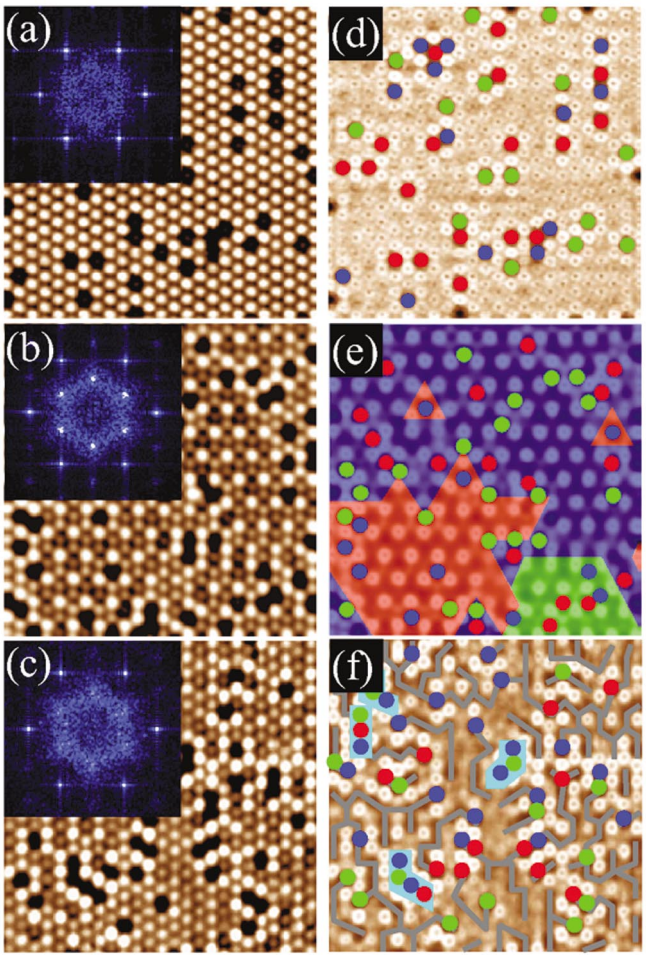

FIG. 1 (color). STM images (14×14 nm^2) of the Pb/Ge interface at (a) RT, (b) 90 K, and (c) 41 K. STM images presented were obtained with the tip bias at +1.5 V and feedback current at 3 nA. The FTs are shown as insets of the corresponding real space images. (d)–(f) show the perpendicular distortion by filtering out the $(\sqrt{3} \times \sqrt{3})$ symmetry from images (a)–(c), respectively. Ge substitutional defects are marked with red, green, or blue circles depending on their coordination relative to the three nonequivalent sites in a (3×3) lattice. In (e), the (3×3) domains are highlighted in colors following the up sites. Three or more neighboring defects are marked in light blue in (f), and the adatoms distorted downwards are connected with gray lines.

Upon cooling, the Pb atoms display an ordered vertical distortion producing (3×3) symmetry at about 110 K [Fig. 1(b)]. The STM image represents the *one up-two down* configuration (*one bright-two dark* in the filled-state image). The (3×3) phase is stable between 110 and 80 K characterized with sharp domain walls and large domain size of $\sim 10 \times 10$ nm^2. As the temperature is further decreased, the (3×3) domains start to shrink and the domain walls dissolve. In Fig. 1(c), the Pb atoms show a disordered structure at 41 K in which the Pb atoms are at randomly distributed height with no apparent LRO [19]. Unlike in the (3×3) phase, no preferred positions (perpendicular distortion) can be identified in the disordered phase since the Pb atoms show a continuous distribution of heights in STM. Both transitions from $(\sqrt{3} \times \sqrt{3})$ to (3×3) and from (3×3) to the disordered phase appear to be reversible.

These two phase transitions can be clearly seen in the Fourier transformations (FT) of the real space STM images [insets in Figs. 1(a)–1(c)]. The $(\sqrt{3} \times \sqrt{3})$ hexagon in the FTs appears in all three phases. The substrate holds the horizontal position of Pb atoms in this basic triangular structure. The inner hexagon (3×3) spots in the FT are weak and fuzzy for the "flat" $(\sqrt{3} \times \sqrt{3})$ surface at RT, turning sharp for the surface buckled with (3×3) LRO, and become fuzzy again for the randomly corrugated surface at 41 K. The presence of defects in the interface results in the enhancement of the (3×3) symmetry at all temperatures, which will be discussed subsequently.

To focus attention on the vertical distortions in the STM images, the $(\sqrt{3} \times \sqrt{3})$ spots in the FT are removed. The transform back to real space is shown in Figs. 1(d)–1(f). At RT [Fig. 1(d)], all the Pb atoms are equivalent except small distortions pinned around defects. This local distortion has the same characteristic as reported for the Sn/Ge system [15,16,18]. At 90 K in Fig. 1(e), large (3×3) domains and sharp domain walls are present, indicating the new LRO is fully developed. In the disordered phase at 41 K, there is no apparent LRO and the configuration of the distorted Pb atoms can be best described as kinked lines, which is indicated by the gray lines in Fig. 1(f).

Two order parameters are defined to quantify these two transitions. First, the atomic roughness (ΔZ), which is defined as the standard deviation of adatom heights seen by the STM, distinguishes the flat $(\sqrt{3} \times \sqrt{3})$ phase and the distorted phases at LT. As shown in the upper panel of Fig. 2, the order parameter $\Delta Z(T)$ increases continuously upon cooling followed by a saturation. The abrupt change of the order parameter expected in a phase transition is absent due to the presence of defects that induce local distortions in the lattice. The transition temperature is estimated from the kink point of the temperature dependence of ΔZ, and yields $T_1 \sim 112$ K. The magnitude of ΔZ is three times larger than that determined by the surface x-ray diffraction analysis [9], indicating that the charge redistribution is more dramatic than the lattice distortion.

The second order parameter is $I_3/I_{\sqrt{3}}$, defined as the intensity ratio between the (3×3) and $(\sqrt{3} \times \sqrt{3})$ spots in the FT of the real space image. This order parameter will distinguish the (3×3) phase from the disordered phase at LT. As shown in the lower panel of Fig. 2, $I_3/I_{\sqrt{3}}$ decreases upon cooling below $T_2 \sim 76$ K, signifying the disappearing of the (3×3) LRO and the onset of the disordered phase. $I_3/I_{\sqrt{3}}$ also indicates the same T_1 for the $(\sqrt{3} \times \sqrt{3})$ to (3×3) phase transition as seen in $\Delta Z(T)$.

It has been documented that the $(\sqrt{3} \times \sqrt{3})$ to (3×3) transition, especially for the Sn/Ge system, is influenced

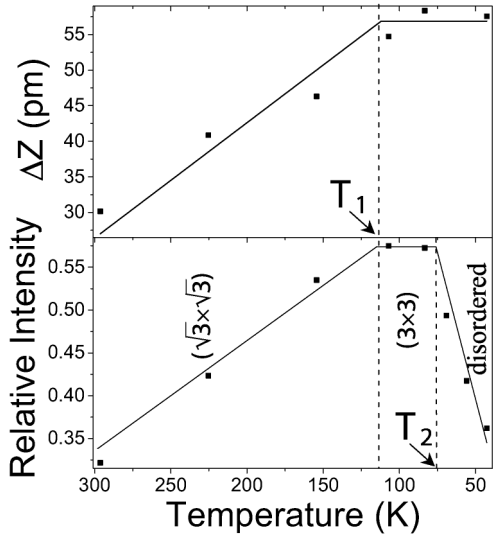

FIG. 2. Temperature dependence of the two order parameters of Pb/Ge interface $\Delta Z(T)$ and $I_3/I_{\sqrt{3}}(T)$. The height Z was obtained with the tip bias at +1.5 V and feedback current at 3 nA.

by defects [15–18]. A quick survey of our STM images reveals that defects are behaving similarly for the Pb/Ge system. Figure 1(d) shows a honeycomb structure developing around the Ge defects. The range of this defect induced density wave is temperature dependent [18] and is responsible for the high temperature tail seen in both order parameters ΔZ and $I_3/I_{\sqrt{3}}$, blurring the clear definition of T_1. When the system enters into the global (3×3) phase below T_1, the defects develop a correlation between themselves in such a way that almost all defects are aligned to the ''down'' sites (the charge-minimum sites) within the (3×3) domains, as previously reported as the ''defect-ordering transition'' in the Sn/Ge interface [18]. Such a correlation between defects can be clearly seen in Fig. 1(e), which shows that all the defects are either isolated or forming pairs, compatible to the (3×3) LRO with *one up-two down* configuration within each domain (red, green, or blue). Figure 1(f) shows that there is a defect induced local distortion at 40 K but it is quite different. First, the defects seem to have lost their alignment within domains as seen in Fig. 1(e), probably because the domain size is very small. Second, it is clear that there is a distinct configuration in which three or more defects may sit side by side and are arranged to ''lines'' or kinked lines, as highlighted in Fig. 1(f). Such a change of the defect distribution indicates that the defects have again moved to accommodate the configuration in the disordered phase.

It is important to clarify the issue whether the observed disordered phase is an intrinsic behavior of the Pb/Ge interface or an effect determined by the defects. These measurements indicate that the defects move on the surface to accommodate the lowest energy configuration for each phase: random in the $(\sqrt{3} \times \sqrt{3})$, ordered within a domain for the (3×3), and in a kinked-line configuration for the disordered phase.

The intrinsic change of the Pb/Ge interface structure becomes clearer by examining the responses of the underlying lattice to defects in different phases. In Fig. 3, we show two areas in the (3×3) phase at 90 K (left) and the disordered phase at 40 K (right), respectively. Both areas are in the same size and have the same number of defects. In the (3×3) phase, a large (3×3) single domain is pinned around the eight defects with distribution compatible to the *one up-two down* configuration. The local distortion around defects is in harmony with the global lattice structure as evident in the left panel of Fig. 3. On the other hand, the right panel of Fig. 3 shows that the kinked-line structure is developed at LT in the area with eight defects even though a single (3×3) domain could accommodate all of them. This comparison clearly demonstrates that the disordered structure is intrinsically a new phase determined by temperature only but not defects. It is important to point out that such a defect distribution is not representative at LT and corresponding to a small portion of defects not fully relaxed to equilibrium sites in the interface due to the finite cooling rate in the experiments. These unrelaxed defects result in a frustrated local configuration around them in the disordered phase (see the right panel of Fig. 3), while in the (3×3) phase, ''unrelaxed'' defects sit on the ''up'' sites of the lattice and are responsible for the domain walls [see Fig. 1(e)].

Existence of the disordered phase at LT unambiguously indicates the frustration arises from different driving forces, none of which is favored by the LT. With a quasiclassical continuum study, Stojković *et al* [3] explained the formation mechanism of various phases in layered transition metal oxides as the competition between the short-range dipolar forces generated by the antiferromagnetic (AF) fluctuations and the long-range Coulomb forces. At

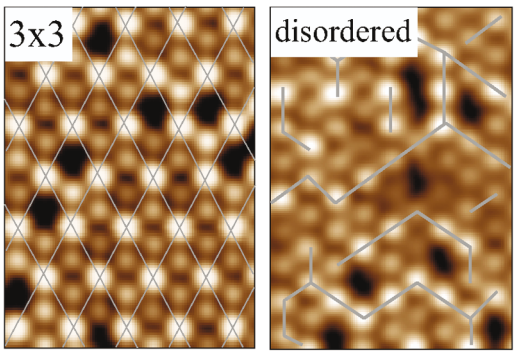

FIG. 3 (color). STM images of a (3×3) single domain at 90 K and an area in the disordered phase at 40 K with the same defect distribution with respect to the virtual (3×3) lattice. The gray grids in the left panel mark the charge-maximum sites of the (3×3) lattice. The kinked-lines structure is indicated in the right panel by the gray lines connecting the adatoms distorted upwards.

certain conditions, the competing length scales lead to rugged free energy profiles in configuration space. LRO is practically unreachable in the system due to the presence of many metastable states.

This model also describes the natural scenario in other 2D systems such as metal-adsorbed semiconductor surfaces. In a separate work, Shi *et al* [1] proposed that the adatom-adatom interaction together with the local stress field are responsible for the $(\sqrt{3} \times \sqrt{3})$ to (3×3) structural phase transition at Sn/Ge or Pb/Ge interface. The motion of adatoms is coupled with the motion of electrons (electron-phonon coupling) in the 2D metallic system so that the indirect adatom-adatom interaction arises. Moving down an adatom repels electrons from the lattice site and the excess electrons are absorbed by the neighboring adatoms, rendering them to move up. This results in a repulsive interaction between the neighboring adatoms. This indirect adatom-adatom interaction mediated by the conduction electrons is essentially the long-range interaction. The short-range and dipolar forces are included in the elastic energy of the lattice distortion that represents the local stress field imposed by the substrate registry. When the long-range interaction overwhelms the short-range interaction that keeps the Pb atoms undistorted, a structural phase transition occurs. The transition is accompanied by the surface charge redistribution with more electrons at up sites and less electrons at down sites, which is consistent with our observation that the distortion observed in STM is much larger than that determined from surface x-ray diffraction analysis [9].

Furthermore, the new phase stabilized at LT could be the (3×3) phase or the glassy phase depending on the relative strength of the two driving forces at different length scales. The glassy phase occurs when the long-range interaction is much stronger than the local stress. In this limit, the system can be mapped to an AF spin Ising model. Simplifying the perpendicular distortion of the adatoms into up or down relatively to their average height without counting the distortion quantitatively, the structural up (down) adatoms are corresponding to the spin-up (spin-down) while the repulsive electron-mediated adatom-adatom interactions are corresponding to the AF coupling between spinons. It is well known that an AF Ising system shows frustration in a triangular $(\sqrt{3} \times \sqrt{3})$ lattice with kinked-line arrangement of spins [20], exactly what we have observed in the corresponding Pb/Ge thin film system at LT. A recent LEED study on Si(001) surface [21] also observed the disappearance of the $c(4 \times 2)$ LRO at LT. Although such a simple geometric frustration cannot be satisfied in the square lattice, the competition between the two length scales is still determinative on the surface structure.

In summary, we observe a structural phase transition from the ordered (3×3) phase to the disordered glasslike phase at ~76 K on Pb/Ge(111) surface. Although blurred by the presence of defects, the transition is demonstrated to be intrinsic by the direct STM imaging. The observation of the new LT disordered phase reveals the intricate competitions between different driving forces of surface reconstruction and their inherent complexity. The ultrathin metallic film on a semiconducting substrate like the Pb/Ge interface provides an ideal platform for understanding these forces in an accessible and controlled way, offering insight into a much broader class of correlated electron systems.

The authors are grateful to the discussions with A. V. Melechko, Jiandi Zhang, and Zhenyu Zhang. This work is funded by NSF Grant No. DMR-0105232. Oak Ridge National Laboratory is managed by UT-Battelle, LLC, for the U. S. Department of Energy under Contract No. DE-AC05-00OR22725.

[1] J. Shi *et al.*, Phys. Rev. Lett. **91**, 76103 (2003).
[2] Branko P. Stojkovoć *et al.*, Phys. Rev. Lett. **82**, 4679 (1999).
[3] Branko P. Stojkovoć *et al.*, Phys. Rev. B **62**, 4353 (2000).
[4] Zohar Nussinov *et al.*, cond-matt/0409474.
[5] J. M. Carpinelli *et al.*, Nature (London) **381**, 398 (1996).
[6] See a recent review in T.-C. Chiang *et al.*, J. Phys. Condens. Matter **14**, R1 (2002).
[7] G. Le Lay *et al.*, Appl. Surf. Sci. **123/124**, 440 (1998).
[8] R. I. G. Uhrberg and T. Balasubramanian, Phys. Rev. Lett. **81**, 2108 (1998).
[9] O. Bunk *et al.*, Phys. Rev. Lett. **83**, 2226 (1999).
[10] J. Zhang *et al.*, Phys. Rev. B **60**, 2860 (1999).
[11] R. Pérez *et al.*, Phys. Rev. Lett. **86**, 4891 (2001).
[12] José Ortega *et al.*, J. Phys. Condens. Matter **14**, 5979 (2002).
[13] G. Santoro *et al.*, Comput. Mater. Sci. **20**, 343 (2001).
[14] S. de Gironcoli *et al.*, Surf. Sci. **454-456**, 172 (2000).
[15] H. H. Weitering *et al.*, Science **285**, 2107 (1999).
[16] L. Petersen *et al.*, Phys. Rev. B **65**, 020101 (2002).
[17] T. E. Kidd *et al.*, Phys. Rev. Lett. **85**, 3684 (2000).
[18] A. V. Melechko *et al.*, Phys. Rev. B **61**, 2235 (2000).
[19] As evident of the absence of LRO, no sharp domain walls are visualized below T_2. But in some rare cases, small (3×3) areas with the diameter up to 3 nm are observed as low as ~60 K, which is compatible with Ref. [5]. In our sample, the slightly higher defect density might further increase the transition temperature to the disordered phase.
[20] K. H. Fischer and J. A. Hertz, *Spin Glasses* (Cambridge University Press, Cambridge, England, 1991).
[21] M. Matsumoto *et al.*, Phys. Rev. Lett. **90**, 106103 (2003).